Measuring the Impact of Road Removal on Vehicular CO2 Emissions

Simone Baccile[1], Giuliano Cornacchia[2] and Luca Pappalardo[3]

[1]University of Pisa, Pisa, Italy
[2]University of Pisa, ISTI-CNR, Pisa, Italy
[3]ISTI-CNR, Scuola Normale Superiore, Pisa, Italy

Abstract
Transportation networks face escalating challenges to cater to increased mobility demand while addressing traffic congestion. Traditional remedies, such as adding roads, can paradoxically worsen congestion, as seen in Braess's paradox. This study emphasizes the potential benefits of strategically closing roads to alleviate congestion and carbon emissions. Milan serves as a case study, where various road closure strategies were tested to identify scenarios where strategic removal not only eased congestion but also significantly reduced CO2 emissions. The findings provide practical insights for urban planners and policymakers, offering a roadmap to develop more efficient and eco-friendly urban transportation systems.

Keywords
CO2 emission, air pollution, mobility, urban simulation, urban sustainability, SUMO, braess paradox

1. Introduction

Traffic congestion is one of the most pressing problems in urban traffic management, increasing air pollution and greenhouse gas emissions [1, 2]. Although several policies have been applied so far to mitigate these issues [3, 4], evaluating their effectiveness is challenging because the interaction between the road network and the mobility demand is non-linear, making it hard to predict the behavior of numerous agents. This non-linearity stems from various factors, such as varying traffic volumes, road conditions, and driver behaviors.

The complexity of the urban system can result in phenomena like Braess's paradox [5, 6, 7, 8]: adding roads may inadvertently exacerbate congestion because each driver, aiming to minimize travel time, may contribute to slowdown traffic rather than alleviate it. The Braess paradox has been studied on toy examples and validated empirically in several cities and through simulations [6, 7, 8]. In the real world, adding a new road requires a thorough analysis of physical space, the available land, terrain characteristics, and the integration with the existing road network. In this study, we focus on road closure since it is a less invasive and easy-to-make process. We assess the impact of road closure on urban CO2 emissions in Milan, Italy, assuming that closing a road may have beneficial effects, leading to a more uniform distribution of traffic across the remaining available roads.

To evaluate the effects of road closures on CO2 emissions, we use SUMO [9], an open-source and widely used microscopic traffic simulator that allows for controlling different aspects of urban traffic, intervening in the road network, and simulating the impact of these interventions in terms of CO2 emissions.

Our analysis reveals roads that, if removed, could reduce CO2 emissions by approximately 10%, as well as roads whose removal could result in an alarming increase in emissions of nearly 50%. Our work provides valuable insights and enables policymakers and city planners to analyze the potential outcomes of various road closure strategies through what-if scenarios.

The code for full replication of this work at https://github.com/Simoniuss/Braess-Paradox-Framework.

2. Related Work

The Braess paradox (BP) [5] states that adding one or more roads to a road network can cause a redistribution of the traffic flow such that the overall travel time increases. When the road network is small, the BP can be solved as a convex optimization problem [10, 11, 12]. When the road network is large, as in the case of real-world road networks, the BP does not necessarily take place, i.e., adding a new road is not always detrimental [13].

Various studies have explored the impact of road closure. In [14], the authors employed convex optimization techniques to reveal that certain routes in Montgomery County could lead to decreased travel times for drivers if closed. In [15], the authors identified roads using heuristic with a genetic algorithm in Winnipeg (Canada), whose removal can reduce the total travel time by 12%. Other studies focus on toy examples, modifying the type of agents, or incorporating additional informa-

Published in the Proceedings of the Workshops of the EDBT/ICDT 2024 Joint Conference (March 25-28, 2024), Paestum, Italy
s.baccile@studenti.unipi.it (S. Baccile);
giuliano.cornacchia@phd.unipi.it (G. Cornacchia);
luca.pappalardo@isti.cnr.it (L. Pappalardo)

tion: Buscema et al. [6], add a line of sight to choose a route in NetLogo, Faccin et al. [16] use Belief-Desire-Intention agents to soften the BP effect, Zhuang et al. [7] explore the effects in a dynamic traffic case, Ziemke and Nagel [17] simulate vehicular traffic using MATSim.

In Barcelona, Sánchez-Vaquerizo and Helbing [8] discovered using SUMO that closing a few roads just to a certain type of vehicle can reduce travel time by 14% and the emissions by 8%. Padrón et al. [18] perform a simulation in SUMO and find that, in Valencia, closing one of the major roads increases CO2 emissions by 3-4%. Other policies try to mitigate urban CO2 emissions, encouraging public transport, creating green areas, and reducing heavy-duty vehicles [19]. A notable example is the "three-in-one" policy applied in Jakarta [20], requiring all private cars, during peak hours, carrying at least three passengers to cross major roads. After the policy was abandoned, there was an increase in delays from 2.8 to 5.3 minutes per km during peak hours.

3. Simulation Framework

Our simulation framework generates urban traffic scenarios under various road closure strategies. The framework consists of two phases, each serving a specific purpose. The first phase simulates urban traffic under normal conditions without road closures (*baseline*). The second phase simulates vehicular traffic by systematically closing one or more roads through diverse closure strategies.

Road network. We model the road network as a directed graph $G = (N, E)$ where the set of edges E contains the road or the streets, and the set of nodes N contains the intersections (junctions) between roads. Each road may be composed of multiple edges, i.e., distinct segments of roads distinguished by specific attributes. We aggregate edges in roads using road names. Given that some edges are without road names and the lack of a standardized naming criterion, we apply the following preprocessing steps:

- Each unnamed edge e has an incoming and an outgoing edge, with their respective road names. If those two road names are the same, we assign that name to e.
- We use the ArcGIS service to get the midpoint coordinates (latitude, longitude) of each unnamed edge using reverse geocoding, thus obtaining the missing road name.
- Since the road network may include more than one municipality, there may be some edges with the same name (aggregated as roads) but geographically distant from each other. We identify these roads using the boundaries of municipalities and assign to each edge its name and the corresponding municipality.
- Some contiguous edges are named with different names (pseudonyms) but are the same road. We cannot automatically change these names because they are culturally or regionally dependent, so after detection, we change them manually.

Mobility demand. We model the vehicle flows through the city's mobility demand where a pair *(o,d)* identifies each vehicle's trip definition, representing the origin and destination location. First, we divide the urban environment into tiles, each of which will be a possible origin or destination location. We choose hexagonal tessellation H3 developed by Uber and available in library scikit-mobility [21]. Then, we use real mobility data, such as vehicles' GPS traces, to estimate the flows between tiles. In practice, we build an Origin-Destination (OD) matrix where an element indicates the number of vehicle trips from an origin tile to a destination tile.

Routes. For each (e_o, e_d) pair in the mobility demand, we use a routing algorithm from SUMO, called Duarouter[1], that connects two edges on a road network following the fastest path, i.e., the path that minimizes the expected travel time. The fastest path can be perturbed using a randomization parameter $w \in [1, +\infty)$ where the higher the w, the more the path is randomized ($w = 1$ is exactly the fastest path). Duarouter dynamically distorts edge weights (i.e., travel time) by a chosen random factor drawn uniformly in $[1, w)$. A w value greater than 1 allows us to model imperfections in human driving behavior, reflecting the lack of complete knowledge of the road network while driving.

Traffic simulation. We generate traffic from the vehicle routes using SUMO (Simulation of Urban MObility) [9]. SUMO is a microscopic model, which means that each vehicle is modelled explicitly, has its route, and moves individually through the network. We estimate CO2 emissions using the HBEFA4 model inspired by the Handbook of Emission Factors from Road Transport [22]. HBEFA4 provides emission factors for a wide list of vehicle types, different pollutants, and several traffic situations. We use this model through the SUMO simulator, which automatically compute the CO2 (mg) emissions for each vehicle.

Road closure. To simulate the effects of road closures on CO2 emissions, we define a road closure simulation framework that allows us to select a set of roads and remove them from the road network, maintaining the mobility demand as similar as possible. The steps of the framework are the following:

1. Select a set of roads to close.
2. Modify the edge parameters in the road network using the "disallow" SUMO attribute to prevent the passage of vehicles on the roads from being closed.

[1] https://sumo.dlr.de/docs/duarouter.html

3. Recompute the mobility demand. We iterate through all the (e_o, e_d) pairs and see if the vehicle trip needs to be changed or not as follows:
    - If e_o or e_d belongs to an edge of the removed roads, we recompute a new trip for that vehicle.
    - If e_o and e_d are not removed from the road, we verify if the two edges are still reachable after the road closure. If so, we keep the vehicle's trip of the baseline mobility demand.
    - If the two edges are no longer connected, we recompute a new trip.
4. Compute the routes for all the vehicles again, considering the new mobility demand.
5. Simulate traffic and gather results: we run a SUMO simulation on the new road network with road closures and recomputed routed paths. Then, we collect the results on CO2 emissions.

4. Road Classification

Inspired by previous works [23, 24], we classify roads using a combination of theoretical measures derived from graph theory, such as betweenness centrality, and data-driven metrics like Volume-Over-Capacity (VOC) and K_{road}, a metric indicating the degree of road usage.

Road betweenness centrality. It is a theoretical measure of centrality in a graph (road network) based on the shortest paths. For our aim, we use the edge betweenness centrality [25, 26] to obtain the road betweenness centrality using a weighted average with the length of the edge as weight:

$$BC(road) = \frac{\sum_{e \in road} BC(e) \cdot length(e)}{\sum_{e \in road} length(e)} \tag{1}$$

where $road$ is the road on which to compute the betweenness, and it is composed of multiple edges e, and $length(e)$ represents the length of the edge e.

Volume-Over-Capacity. The Volume-Over-Capacity (VOC) is the ratio between the traffic flow on a road and the capacity of the road. It is a standard metric to evaluate a road's service level and indicates how congested a road is [27, 28]. When $VOC < 1$, the road can still contain other vehicles without undergoing particular slowdowns. A road with $VOC \geq 1$ suffers from congestion.

First, we compute the VOC to the edge level and then aggregate them to the road level. We compute the volume edge of each road segment using a data-driven approach, running a SUMO simulation with the mobility demand derived from the GPS data.

In the absence of the actual capacities of the roads, we estimated them using the 2000 Highway Capacity Manual [29]. Then, we compute the VOC for each edge as:

$$VOC(e) = \frac{V(e)}{C(e)} \tag{2}$$

To obtain the VOC associated with each road, we compute the weighted average of the VOC of each edge in the road:

$$VOC(road) = \frac{\sum_{e \in road} VOC(e) \cdot length(e)}{\sum_{e \in road} length(e)} \tag{3}$$

where a $road$ is composed by multiple edges e.

$\mathbf{K_{road}}$. The K_{road} is a metric that measures the attractiveness of each road segment. It quantifies how many city areas (neighborhoods or tiles) contribute the most to the traffic flow on that specific road segment [24]. To compute the K_{road} of each edge in the road network, we first need to define the network of road usage, a bipartite network where each road edge e is connected to its major driver areas. The major driver areas are the ranked neighborhoods that produce 80% of the traffic flow for an edge.

We develop two concept related to the K_{road}, the $K_{road}^{(source)}$ and the $K_{road}^{(dest)}$. An area T is a driver source for an edge e if at least one vehicle, which passes through the edge e, starts its trip from an edge $e_s \in T$. Similarly, an area T is a driver destination for e if at least one vehicle, which passes through the edge e, ends its trip to an edge $e_d \in T$. An area can be both a source and a destination. For each edge, e, the driver sources and driver destinations can be ranked based on how many vehicles traverse e, starting or ending in the respective area.

We compute the weight of each driver source as follows:

$$I_{e,T}^{(source)}(v) = \begin{cases} 1 & \text{if } v \text{ passes through } e \text{ from } T \\ 0 & \text{otherwise} \end{cases} \tag{4}$$

$$DS_e(T) = \sum_{v \in V} I_{e,T}^{(source)}(v) \tag{5}$$

where e is the edge on which compute the driver sources, T is a neighborhood, and V is the set of vehicles crossing the city. Similarly, we can define the driver destinations $DD_e(T)$. We rank the list of driver sources (DS) and driver destinations (DD) for each edge and keep only the DS and the DD responsible for 80% of the traffic flow on the edge. These new lists are the major driver sources (MDS) and the major driver destinations (MDD) for each edge e. After identifying the MDS and the MDD, we can build the bipartite road usage networkFinally, we compute $K_{road}^{(source)}$ and $K_{road}^{(dest)}$ from the bipartite network BG:

$$K_{road}^{(source)}(e) = |\{l \mid \exists e \xleftarrow{l} T, \forall\, T \in A,\ l \in L\}| \quad (6)$$

$$K_{road}^{(dest)}(e) = |\{l \mid \exists e \xrightarrow{l} T, \forall\, T \in A,\ l \in L\}| \quad (7)$$

where A is the set of area-nodes of the bipartite graph BG, L is the set of links of BG, e is an edge $\in E$ the set of edge-nodes of the bipartite graph, and l is an in-going or an out-going link from an area-node T. Actually, $K_{road}^{(source)}$ and $K_{road}^{(dest)}$ are respectively the in-degree and the out-degree of each $e \in E$ of the bipartite graph. Ultimately, we aggregate these measures to road level with a weighted average using the length of each edge as weight.

Road clustering. We use a clustering approach to divide the roads into categories and obtain an effective closure strategy to evaluate the impact on CO2 emissions. We use the road betweenness centrality, the VOC, $K_{road}^{(source)}$, and the $K_{road}^{(dest)}$ as features for clustering to obtain several road categories. We use the K-Means clustering[2] to group the roads and a grid search to find the optimal number of clusters.

We test $k = 2, \ldots, 10$, choosing the best k using the elbow method [30].

5. Closure Strategies

We design different road closure strategies and evaluate their impact on CO2 emissions.

CO2 policy. It removes roads based on their level of CO2 emissions. We normalize emissions by road length, obtaining CO2 per meter of road.

Category policy. It closes roads based on a classification of roads. We analyze the impact of CO2 emissions when roads are closed from each category, closing roads with the highest CO2 per meter first.

Mixed policy. We choose a list of roads for removal, ensuring that it comprises an equal number of roads from every category. These roads were ranked in descending order based on their CO2 emissions per meter in each category. Initially, we eliminate the road with the highest emissions within each category, progressively working towards those with lower emissions. As an example, consider three road categories denoted as $A = [a_1, a_2, a_3, a_4], B = [b_1, b_2, b_3, b_4], C = [c_1, c_2, c_3, c_4]$, where each list is arranged in decreasing order of CO2/m. If we aim to remove six roads, the list of removed roads would be $R = [a_1, a_2, b_1, b_2, c_1, c_2]$, such that the list R has the same amount of roads from each category.

The rationale behind employing a mixed strategy lies in the road categorization based on their significance or attractiveness in the network. This approach increases the likelihood of obtaining clusters with similar types of roads, such as highways or freeways. Simply removing all roads from a single category may have a detrimental impact because vehicles previously using those roads are now directed to alternative routes lacking similar characteristics, such as reduced capacity or lower speed limits. Therefore, removing roads from diverse categories helps mitigate this effect.

[2]https://scikit-learn.org/stable/modules/clustering.html

6. Experimental Setup

Road Network. We apply the simulation framework to a squared area of almost $380\ km^2$ from the centre of Milan and download the corresponding road network from OpenStreetMap, obtaining $24,063$ intersections and $46,488$ edges, which we aggregate into 7,654 roads.

Mobility Demand. We split the selected area into tiles using H3 hexagonal tessellation with a resolution of 8, covering the selected Milan area with 680 tiles. We then use GPS data describing 17,087 vehicles travelling between April 2nd and 8th, 2007 (658k points after preprocessing) to extract the flows of vehicles between tiles. Next, we create a realistic synthetic OD matrix that mirrors real-world mobility patterns, maintaining the typical distribution of trip distances and the power-law behavior in the number of trips between two locations. We compute the mobility demand for $30,000$ vehicles as it minimizes the Jensen-Shannon divergence between the travel time distribution in real data and that of the simulated vehicles [31, 32, 33].

Routes. We generate the routes from the mobility demand using Duarouter, which computes the perturbed fastest path using a randomization parameter $w = 7.5$, which allows us to model the real behavior of drivers who typically do not follow the fastest route [34].

Closure strategy. We simulate the traffic demand using SUMO, obtaining the CO2 emissions for each edge and aggregating the results by road. We first simulate the original road network as a baseline and then select a closure strategy to remove a set of roads from the original road network. A closure strategy consists of two parallel steps. The first is the informed strategy, where we remove the roads from the road network based on the defined strategy. The second is an uninformed policy in which we close random roads from the road network. The removed roads in the uninformed strategy preserve the same length as the informed one. For each policy, we close 1, 10, 20, …, 100 roads. Independently of the policy applied, the road closures are selected with respect to the baseline experiment, the original road network. Thus, each set of roads is a subset of the next set $1 \subseteq 10 \subseteq 20 \subseteq \ldots \subseteq 100$. We rank roads within each strategy based on their CO2/m in descending order. Subsequently, we incrementally select the set of roads for closure, employing a precise approach to optimize the reduction of carbon emissions. While this decision is inherent in the CO2 policy by its definition, for both the category and mixed policies, we follow the strategy outlined in Section 5. This involves ranking roads based on emission levels (CO2/m) in descending order and prioritizing the closure of the most polluted roads from each road category.

Road classification. We classify the roads of Milan to identify similarities and differences between roads that can be impactful in terms of CO2 (mg) emissions. As suggested in [24], we characterize roads with their betweenness centrality and $K_{road}^{(source)}$ [24], as well as additional features such as the VOC, a useful metric to classify to quantify road congestion, and $K_{road}^{(dest)}$ to capture the attractiveness of each road based on the destination of the flows. We then apply a clustering algorithm using the Silhouette score's progression to determine that the best number of clusters is four. We name the clusters as follows:

- **(HF)**: High K_{road}, high relative VOC and emissions (in yellow);
- **(HE)**: High K_{road}, low relative VOC and emissions (in green);
- **(LF)**: Low K_{road}, high relative VOC and emissions (in orange);
- **(LE)**: Low K_{road}, low relative VOC and emissions (grey).

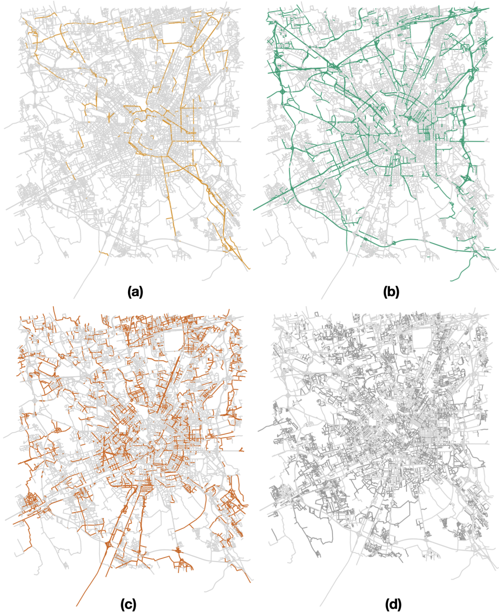

Figure 1: Road distribution of each category defined from the classification of the roads in the road network of Milan. (a)-(b) Roads with high K_{road}. (c)-(d) Roads with low K_{road}.

First, we run a SUMO simulation on the original Milan road network, i.e., without any road closure. Through this simulation, we identify the roads with higher emissions levels. Figure 1 shows the roads from each cluster previously identified for the K_{road} and the mixed policy. In Figure 1a and 1b, we observe the roads characterized by high $K_{road}^{(source)}$ and $K_{road}^{(dest)}$. The yellow roads within these figures can be differentiated from the green roads based on their CO2/m (mg/m) and VOC levels. Notably, the yellow roads exhibit higher levels of both CO2/m and VOC than the green roads. In Figure 1c and 1d, we show the roads classified with low K_{road}. We can distinguish between two groups based on their VOC values: high VOC for the orange roads and low for the dark grey roads.

7. Results

Figure 2 provides an overview of total CO2 emissions (mg) across the entire road network for each applied closure strategy. Now, we discuss each policy individually.

CO2 policy. It exhibits a beneficial impact on reducing CO2 emissions up to a certain threshold (Figure 2a). Closing up to 50 roads leads to a decrease in the overall emission compared to the baseline scenario. After this threshold, the emissions increase exponentially with the closing of every additional set of ten roads. The CO2 policy also highlights that an informed strategy based on the level of CO2/m is more effective than an uninformed strategy with the same emissions level as the baseline.

Category policy. The impact of this policy depends on the road category. Closing HF roads (Figure 2b) leads to similar results to the CO2 policy: there are beneficial effects until a certain threshold (40 closed roads). After closing 100 HF roads, CO2 emissions decrease, even if remaining above the baseline level. After closing 50 roads, the random closure strategy outperforms the informed strategy regarding CO2 emissions, although still worst concerning the baseline. Closing HE roads (Figure 2c) consistently results in a negative impact, with CO2 emissions increasing up to 50% above the baseline. Even in the case of the uninformed strategy, emissions levels rise, although to a lesser extent. Closing LF roads (Figure 2d) always leads to an increase in CO2 emissions, although to a lesser degree than other removal strategies. The closed roads cause a maximum increase of 15% compared to the baseline. Lastly, closing LE roads does not change emissions levels compared to the baseline (Figure 2e).

Mixed policy. Even if the impact of this policy does not exhibit a clear trend (Figure 2f), it is worse compared to the baseline scenario. Focusing on the closure experiment of 20 roads, we find no linear relationship between the roads closed and the resulting CO2 emissions.

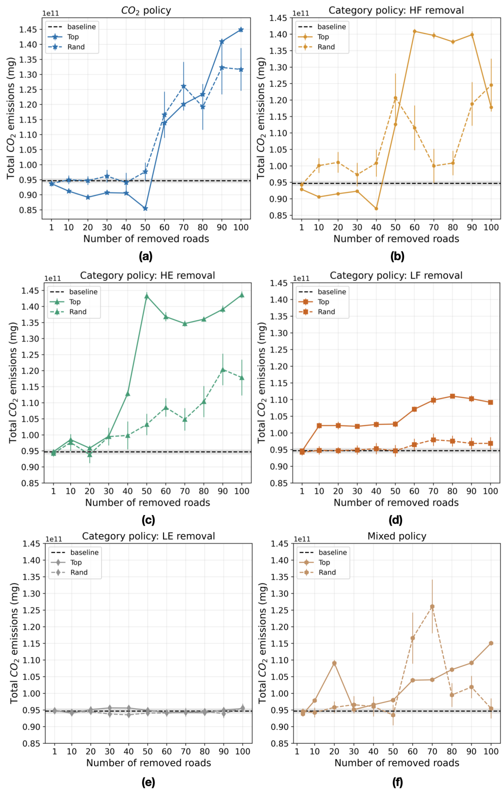

Figure 2: The results on CO2 emissions (mg) obtained from different road closure strategies. (a) CO2 policy. (b-e) Category policy. (f) Mixed policy.

Comparing strategies. Figure 3 provides a deeper analysis of the different closure strategies from multiple perspectives. In Figure 3a, we show the percentage of vehicles impacted by each closure strategy. A vehicle is considered impacted if its previous route contains at least one road closed in the closure strategy. The closure of HE roads yields a higher percentage of impacted vehicles due to two key factors. Firstly, HE roads encompass highly frequented routes, including highways, which affect a larger proportion of vehicles. Secondly, HE roads comprise a larger number of roads, some longer, thereby amplifying the impact on vehicle paths.

Figure 3b shows the percentage of the traveled road network to the total available road network. In theory, the more vehicles are spread on the road networks, the fewer the emissions as we reduce the likelihood of road congestion. However, this effect is not observed because we are not simply redistributing the vehicles through the road network but also removing roads from it. Road removal limits the available route options for drivers, leading to a situation that replicates or worsens the initial conditions.

To gain insights into the impact of road closures on the routed paths of vehicles, we analyze how the vehicles are rerouted after a closure. Figure 4 shows an example of vehicle rerouting after a road closure. The closed roads are represented in black, while the routed paths are depicted in blue and orange. The orange path represents the routed path in the baseline scenario; the blue path is the rerouted path in the closure experiment. In this case, we consider the CO2 policy with the removal of ten roads. The rerouted path does not differ significantly from the original path because the roads used in the closure experiment have a smaller capacity than the baseline roads. As a result, when simulating all traffic flows, this capacity discrepancy leads to earlier congestion levels.

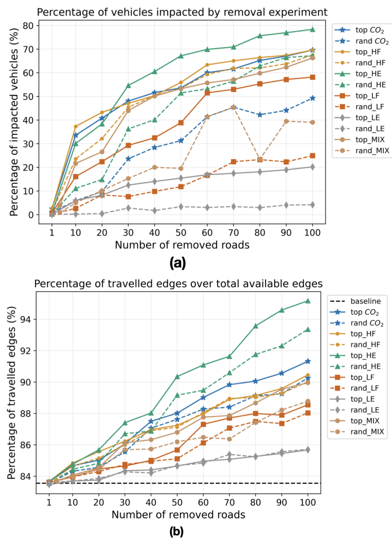

Figure 3: The impact of different road closure strategies on vehicles and the travelled road network edges. (a) Percentage of vehicles impacted by each road closure strategy. (b) Percentage of road network travelled.

7.1. Discussion

Road closures impact CO2 emissions. Emissions decrease for specific road categories up to a certain threshold of removed roads. However, increasing the number of removed roads, CO2 emissions increase exponentially, reaching peaks of 50% above the baseline scenario with the original road network. This happens because highly polluted roads are also typically those with higher capacity, and better equipped to handle larger traffic flows.

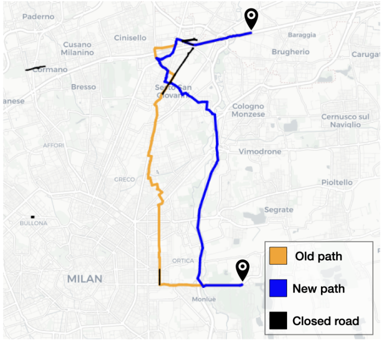

Figure 4: Example of vehicle route change after a road closure. Black roads are the closed ones. In orange is the route of the vehicle before the closure. In blue is the new route considering the closed roads.

Consequently, traffic is rerouted through lower-capacity roads, thus increasing congestion and emissions.

Not all roads count equally. Certain roads are pivotal in maintaining smooth traffic flow and preventing congestion. Those roads cannot be removed without increasing CO2 emissions. We also identify roads whose removal does not significantly affect CO2 emissions.

Removing sparse roads is ineffective. Emissions only decrease for a specific subset of roads, while most closure experiments result in increased emissions. In other words, removing scattered roads throughout the road network may not be optimal. The underlying reason lies in the rerouting of vehicles onto alternative roads, which are often close to the removed roads and have lower capacity. Consequently, this necessitates considering a “zone" closure strategy to mitigate this effect and optimize emissions reduction efforts.

8. Conclusion

Using our simulation framework, we found that closing some roads is beneficial, but the removal becomes detrimental above a certain threshold of closed roads. The closure of other roads led to an increase in CO2 emissions, while certain roads have negligible influence on CO2 emissions. Our work can be further improved in several directions. For instance, another road closure strategy could be to close all roads in specific “eco-zones" rather than closing single roads, which may lead to traffic redirection onto adjacent roads with lower capacity.

Acknowledgements

Questo lavoro è stato finanziato dal PNRR (Piano Nazionale di Ripresa e Resilienza) nell’ambito del programma di ricerca 20224CZ5X4_PE6_PRIN 2022 “URBAI - Urban Artificial Intelligence” (CUP B53D23012770006), Finanziato dall’Unione Europea - Next Generation EU.

This research has also been partially supported by EU project H2020 SoBigData++ G.A. 871042; and NextGenerationEU—National Recovery and Resilience Plan (Piano Nazionale di Ripresa e Resilienza, PNRR), Project “SoBigData.it—Strengthening the Italian RI for Social Mining and Big Data Analytics”, prot. IR0000013, avviso n. 3264 on 28/12/2021.

References

[1] L. Pappalardo, E. Manley, V. Sekara, L. Alessandretti, Future directions in human mobility science, Nature computational science 3 (2023) 588–600.

[2] D. Pedreschi, L. Pappalardo, R. Baeza-Yates, A.-L. Barabasi, F. Dignum, V. Dignum, T. Eliassi-Rad, F. Giannotti, J. Kertesz, A. Knott, Y. Ioannidis, P. Lukowicz, A. Passarella, A. S. Pentland, J. Shawe-Taylor, A. Vespignani, Social ai and the challenges of the human-ai ecosystem, 2023. arXiv:2306.13723.

[3] P. Kuss, K. Nicholas, A dozen effective interventions to reduce car use in european cities: Lessons learned from a meta-analysis and transition management, Case Studies on Transport Policy 10 (2022). doi:10.1016/j.cstp.2022.02.001.

[4] P. Filigrana, J. Levy, J. Gauthier, S. Batterman, S. Adar, Health benefits from cleaner vehicles and increased active transportation in seattle, washington, Journal of Exposure Science & Environmental Epidemiology 32 (2022). doi:10.1038/s41370-022-00423-y.

[5] D. Braess, A. Nagurney, T. Wakolbinger, On a paradox of traffic planning, Transportation Science 39 (2005) 446–450. doi:10.1287/trsc.1050.0127.

[6] D. Buscema, M. Ignaccolo, G. Inturri, A. Pluchino, A. Rapisarda, C. Santoro, S. Tudisco, The impact of real time information on transport network routing through intelligent agent-based simulation, TIC-STH’09: 2009 IEEE Toronto International Conference - Science and Technology for Humanity (2009) 72 – 77. doi:10.1109/TIC-STH.2009.5444404.

[7] D. Zhuang, Y. Huang, V. Jayawardana, J. Zhao, D. Suo, C. Wu, The braess paradox in dynamic traffic, 2022.

[8] J. Argota Sánchez-Vaquerizo, D. Helbing, Less can be more: Pruning street networks for sustainable city making, 2022.

[9] D. Krajzewicz, G. Hertkorn, C. Feld, P. Wagner, Sumo (simulation of urban mobility); an open-source traffic simulation, 2002, pp. 183–187.

[10] T. Roughgarden, Designing networks for selfish

users is hard, 2001, pp. 472– 481. doi:10.1109/SFCS.2001.959923.

[11] Q. Tu, L. Cheng, D. Li, J. Ma, C. Sun, Traffic paradox under different equilibrium conditions considering elastic demand, PROMET - Traffic & Transportation 31 (2019) 1–9. doi:10.7307/ptt.v31i1.2795.

[12] H. Yang, M. Bell, A capacity paradox in network design and how to avoid it, Transportation Research Part A: Policy and Practice 32 (1998) 539–545. doi:10.1016/S0965-8564(98)00017-2.

[13] R. Steinberg, W. Zangwill, The prevalence of braess' paradox, Transportation Science 17 (1983) 301–318. doi:10.1287/trsc.17.3.301.

[14] M. Burov, C. Kizilkale, A. Kurzhanskiy, M. Arcak, Detecting braess routes: an algorithm accounting for queuing delays with an extended graph, 2021.

[15] S. Bagloee, A. Ceder, M. Tavana, C. Bozic, A heuristic methodology to tackle the braess paradox detecting problem tailored for real road networks, Transportmetrica A: Transport Science 10 (2014) 437–456. doi:10.1080/23249935.2013.787557.

[16] J. Faccin, I. Nunes, A. Bazzan, Understanding the behaviour of learning-based bdi agents in the braess' paradox (2017) 187–204. doi:10.1007/978-3-319-64798-2_12.

[17] T. Ziemke, K. Nagel, Braess's paradox in an agent-based transport model, Procedia Computer Science 83 (2016). doi:10.1016/j.procs.2016.04.190.

[18] J. Padrón, M. Terol, J. Zambrano-Martinez, C. Calafate, J.-C. Cano, P. Manzoni, Assessing the impact of road traffic constraints on pollution (2021) 1–5. doi:10.1109/VTC2021-Fall52928.2021.9625237.

[19] H. Zhang, J. Peng, R. Wang, J. Zhang, D. Yu, Spatial planning factors that influence co2 emissions: A systematic literature review, Urban Climate 36 (2021) 100809. doi:10.1016/j.uclim.2021.100809.

[20] R. Hanna, G. Kreindler, B. A. Olken, Citywide effects of high-occupancy vehicle restrictions: Evidence from three-in-one in jakarta, Science 357 (2017) 89–93. doi:10.1126/science.aan2747.

[21] L. Pappalardo, F. Simini, G. Barlacchi, R. Pellungrini, scikit-mobility: A Python Library for the Analysis, Generation, and Risk Assessment of Mobility Data, Journal of Statistical Software 103 (2022) 1–38. URL: https://www.jstatsoft.org/index.php/jss/article/view/v103i04. doi:10.18637/jss.v103.i04.

[22] . Z. Beat Stutzer, Handbook emission factors for road transport, 2023. URL: https://www.hbefa.net/e/index.html.

[23] J. L. Toole, S. Colak, B. Sturt, L. P. Alexander, A. Evsukoff, M. C. González, The path most traveled: Travel demand estimation using big data resources, Transportation Research Part C: Emerging Technologies 58 (2015) 162–177. URL: https://www.sciencedirect.com/science/article/pii/S0968090X15001631. doi:https://doi.org/10.1016/j.trc.2015.04.022, big Data in Transportation and Traffic Engineering.

[24] P. Wang, T. Hunter, A. M. Bayen, K. Schechtner, M. C. González, Understanding road usage patterns in urban areas, Scientific Reports 2 (2012). URL: https://doi.org/10.1038%2Fsrep01001. doi:10.1038/srep01001.

[25] U. Brandes, On variants of shortest-path betweenness centrality and their generic computation, Social Networks 30 (2008) 136–145. doi:https://doi.org/10.1016/j.socnet.2007.11.001.

[26] L. Lu, M. Zhang, Edge Betweenness Centrality, Springer New York, New York, NY, 2013, pp. 647–648. doi:10.1007/978-1-4419-9863-7_874.

[27] O. Hrytsun, Impact of traffic volume and composition on the change in the speed of traffic flow, Transport technologies 2023 (2023) 12–20. doi:10.23939/tt2023.01.012.

[28] D. Othayoth, K. K. Rao, Investigating the relation between level of service and volume-to-capacity ratio at signalized intersections under heterogeneous traffic condition, Transportation Research Procedia 48 (2020) 2929–2944. doi:https://doi.org/10.1016/j.trpro.2020.08.190, recent Advances and Emerging Issues in Transport Research – An Editorial Note for the Selected Proceedings of WCTR 2019 Mumbai.

[29] W. Kittelson, R. Roess, Highway capacity analysis after highway capacity manual 2000, Transportation Research Record 1776 (2001) 10–16. doi:10.3141/1776-02.

[30] H. Humaira, R. Rasyidah, Determining the appropiate cluster number using elbow method for k-means algorithm, 2020. doi:10.4108/eai.24-1-2018.2292388.

[31] G. Cornacchia, M. Böhm, G. Mauro, M. Nanni, D. Pedreschi, L. Pappalardo, How routing strategies impact urban emissions, in: Proceedings of the 30th International Conference on Advances in Geographic Information Systems, 2022, pp. 1–4.

[32] G. Cornacchia, M. Nanni, L. Pappalardo, One-shot traffic assignment with forward-looking penalization, SIGSPATIAL '23, Association for Computing Machinery, New York, NY, USA, 2023. doi:10.1145/3589132.3625637.

[33] G. Cornacchia, M. Nanni, D. Pedreschi, L. Pappalardo, Navigation services and urban sustainability, Fluctuation and Noise Letters (2023) 2450016.

[34] A. Tawfik, S. Miller, Driver route choice behavior: Experiences, perceptions, and choices, 2010, pp. 1195 – 1200. doi:10.1109/IVS.2010.5547968.